

Thermoelastic waves in an anisotropic infinite plate

Hussain Al-Qahtani and Subhendu K. Datta^{a)}

Department of Mechanical Engineering, University of Colorado, Boulder, Colorado 80309-0427

(Received 25 March 2004; accepted 2 June 2004)

An analysis of the propagation of thermoelastic waves in a homogeneous, anisotropic, thermally conducting plate has been presented in the context of the generalized Lord-Shulman theory of thermoelasticity. Three different methods are used in this analysis: two of them are exact and the third is a semianalytic finite element method (SAFE). In our exact analysis, two different approaches are used. The first one, which is applicable to transversely isotropic plate, is based on introducing displacement potential functions, whereas in the second approach, which is applicable to any triclinic material, we rewrite the governing equations and boundary conditions in a matrix form. Finally, in the SAFE method, the plate is discretized along its thickness using N parallel, homogeneous layers, which are perfectly bonded together. Frequency spectrum and dispersion curves are obtained using the three methods and are shown to agree well with each other. The effects of thermal relaxation time and coupling term are also investigated. Numerical calculations have been presented for a silicon nitride (Si_3N_4) plate. However, the methods can be used for other materials as well. © 2004 American Institute of Physics. [DOI: 10.1063/1.1776323]

I. INTRODUCTION

During the second half of the 20th century, nonisothermal problems of the theory of elasticity have been investigated extensively. This is due mainly to their many applications in widely diverse fields. First, in the field of nondestructive evaluation, laser-generated waves have attracted great attention owing to their potential application to noncontact and nondestructive evaluation of sheet materials. Second, the high velocities of modern aircraft give rise to aerodynamic heating, which produces intense thermal stresses, reducing the strength of the aircraft structure. Third, in the nuclear field, the extremely high temperatures and temperature gradients originating inside nuclear reactors influence their design and operations.¹ Moreover, it is well recognized that the investigation of the thermal effects on elastic wave propagation has bearing on many seismological and astrophysical problems.²

Most materials undergo appreciable changes of volume when subjected to variations of the temperature. If thermal expansions or contractions are not freely admitted, temperature variations give rise to thermal stresses. Conversely a change of volume is attended by a change of the temperature. When a given element is compressed or dilated, these volume changes are accompanied by heating and cooling, respectively. The study of the influence of the temperature of an elastic solid upon the distribution of stress and strain, and of the inverse effect of the deformation upon the temperature distribution is the subject of thermoelasticity.³

The classical theory of heat conduction in solids rests upon the hypothesis that the flux of heat is proportional to the gradient of the temperature distribution. As a consequence of this hypothesis, the equation is governed by a parabolic partial differential equation, which predicts that the

application of a thermal disturbance in a body instantaneously affects all points of the body. This assumption of infinite speed is contrary to physical phenomenon. To remove this paradox inherent in the classical theory, a theory of generalized thermoelasticity was developed. This generalized theory accounts for the short time required to establish a steady state heat conduction when a temperature gradient is suddenly produced in the solid. This short time is called the thermal relaxation time. The concept of generalized thermoelasticity has led to a wide range of extensions of the classical theory of thermoelasticity. Various generalization include the following.

- (i) Thermoelasticity proposed by Lord and Shulman in 1967 (L–S model),⁴ in which, in comparison to the classical theory, the Fourier law of heat conduction is modified by taking into consideration a single relaxation time.
- (ii) Thermoelasticity introduced by Green and Lindsay in 1972 (G–L model),⁵ in which the constitutive relations for the stress tensor and the entropy are generalized by introducing two different relaxation times.
- (iii) Thermoelasticity without energy dissipation, proposed by Green and Naghdi in 1992 (G–N model),⁶ in which, the Fourier law is replaced by a heat flux rates–temperature gradient relaxation.

These generalization are the most important ones. For other variations, one can refer for instance to Hetnarski and Ignaczak.⁷

Guided thermoelastic waves were considered by several researchers. Nayfeh and Nemat-Nasser,⁸ Sinha and Sinha,⁹ Agarwal,¹⁰ Sherief and Helmy,¹¹ and Abd-alla and Al-dawry¹² studied isotropic thermoelastic Rayleigh waves. Massalas,¹³ Daimaruya and Naioth,¹⁴ Massalas and Kalpakidis,¹⁵ Sharma, Singh, and Kumar,¹⁶ considered the propagation of

^{a)}Author to whom correspondence should be addressed; electronic mail: dattas@spot.colorado.edu

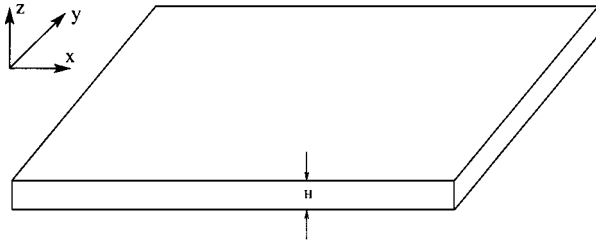


FIG. 1. Geometry of the problem.

guided thermoelastic waves in an isotropic plate. Sharma and Sharma¹⁷ studied the free vibration of a thermoelastic cylindrical panel.

In contrast, little work has been reported on thermoelastic waves in anisotropic plates. The main focus of our work will be on the laser-generated waves in thermoelastic anisotropic plate. As mentioned above, the technique of laser-generated waves has potential application to noncontact and nondestructive evaluation and characterization of sheet materials in industry. It was demonstrated that the thickness of and moduli of thin plates can be measured experimentally using laser-generated waves.¹⁸ In the first part of our work, dispersion relations for thermoelastic anisotropic plate will be studied. These relations are investigated first because of their importance in calculating elastic and thermal properties of materials. Moreover, using dispersion relations, it is then possible to analyze transient response of a plate heated by a laser pulse which will be the subject of our future investigation. The study is carried out in the context of Lord-Shulman (L-S) theory of thermoelasticity using single relaxation time. Two different methods have been used to model the problem. The first is an exact analysis using two different approaches (Secs. II A and II A 2) and a semianalytic finite element method (SAFE) (Sec. II B). Numerical results and discussion are presented in Sec. III. This work concludes with a discussion of possible future work.

II. THEORETICAL FORMULATIONS

We consider an infinite homogeneous transversely isotropic thermally conducting elastic plate at a uniform temperature T_0 in the undisturbed state having a thickness H , see Fig. 1. The motion is assumed to take place in three dimensions (x, y, z). The displacements in the x , y , and z directions are u, v , and w , respectively.

A. Exact analysis

In the absence of body forces and internal heat source the generalized L-S thermoelasticity governing equations are

$$\sigma_{ij,j} = \rho \ddot{u}_i, \quad (1)$$

$$q_{i,j} = -T_0 \rho \dot{\eta}, \quad (2)$$

$$\sigma_{ij} = c_{ijkl} \epsilon_{kl} - \beta_{ij} T, \quad (3)$$

$$\rho \dot{\eta} = \beta_{ij} \dot{\epsilon}_{ij} + \frac{\rho C_E}{T_0} \dot{T}, \quad (4)$$

$$\epsilon_{ij} = \frac{1}{2}(u_{i,j} + u_{j,i}), \quad (5)$$

$$q_i + \tau_0 \dot{q}_i = -K_{ij} T_{,j}. \quad (6)$$

In the above equations, a comma followed by a suffix denotes spatial derivative and a superposed dot denotes the derivative with respect to time.

Various physical variables and material constants appearing in the above equations are the following: σ_{ij} , the components of stress tensor; q_i , the components of heat flux vector; ϵ_{ij} , the components of strain tensor; ρ , mass density; K_{ij} , the coefficients of thermal conductivity; t , time; c_{ijkl} , the elastic constants; η , entropy density; β_{ij} , the thermal coefficients; C_E , the specific heat at constant deformation; T , temperature perturbation; τ_0 , thermal relaxation time; u_i , the components of displacement vector; T_0 , reference temperature ($i, j, k, l = 1, 2, 3$). It is assumed that $|T/T_0| \ll 1$.

In transversely isotropic material and assuming that the x axis is the axis of symmetry of the material, the stresses can be written in terms of the displacements and temperature variation as

$$\sigma_{xx} = c_{11}u_{,x} + c_{12}v_{,y} + c_{12}w_{,z} - \beta_{xx}T, \quad (7)$$

$$\sigma_{yy} = c_{12}u_{,x} + c_{22}v_{,y} + c_{23}w_{,z} - \beta_{yy}T, \quad (8)$$

$$\sigma_{zz} = c_{12}u_{,x} + c_{23}v_{,y} + c_{22}w_{,z} - \beta_{yy}T, \quad (9)$$

$$\sigma_{yz} = c_{44}(v_{,z} + w_{,y}), \quad (10)$$

$$\sigma_{xz} = c_{55}(u_{,z} + w_{,x}), \quad (11)$$

$$\sigma_{xy} = c_{55}(u_{,y} + v_{,x}), \quad (12)$$

where

$$c_{44} = \frac{1}{2}(c_{22} - c_{23})$$

and

$$\beta_{xx} = c_{11}\alpha_{xx} + 2c_{12}\alpha_{yy}, \quad \beta_{yy} = c_{12}\alpha_{xx} + (c_{22} + c_{23})\alpha_{yy}. \quad (13)$$

Here, α_{xx} and α_{yy} are the coefficients of linear thermal expansions in x and y directions, respectively.

By substitution of the foregoing expressions into Eqs. (1)–(6), one can write the governing equations in terms of displacement and temperature,

$$c_{11}u_{,xx} + c_{12}v_{,xy} + c_{12}w_{,xz} + c_{55}(u_{,yy} + v_{,xy}) + c_{55}(u_{,zz} + w_{,xz}) - \beta_{xx}T_{,x} = \rho \ddot{u}, \quad (14)$$

$$c_{55}(u_{,xy} + v_{,xx}) + c_{12}u_{,xy} + c_{22}v_{,yy} + c_{23}w_{,yz} + c_{44}(v_{,zz} + w_{,yz}) - \beta_{yy}T_{,y} = \rho \ddot{v}, \quad (15)$$

$$c_{55}(u_{,xz} + w_{,xx}) + c_{44}(v_{,yz} + w_{,yy}) + c_{12}u_{,xz} + c_{23}u_{,yz} + c_{22}w_{,zz} - \beta_{yy}T_{,z} = \rho \ddot{w}, \quad (16)$$

TABLE I. Some numerical constants for different materials.

Material	v_x ,m/s	k_x ,m ² /s	\bar{K}	$\bar{\beta}$	ε
Aluminum alloy	3.88×10^3	1.02×10^{-11}	1	1	2.56×10^{-3}
Zinc	4.77×10^3	4.45×10^{-5}	1	0.882	2.16×10^{-2}
Silicon nitride	1.34×10^4	2.58×20^{-5}	0.786	0.843	2.49×10^{-3}

$$\begin{aligned}
 &K_{xx}T_{,xx} + K_{yy}T_{,yy} + K_{zz}T_{,zz} - \rho C_E(\dot{T} + \tau_0\ddot{T}) \\
 &= T_0[\beta_{xx}(\dot{u}_{,x} + \tau_0\ddot{u}_{,x}) \\
 &\quad + \beta_{yy}(\dot{v}_{,y} + \tau_0\ddot{v}_{,y}) + \beta_{zz}(\dot{w}_{,z} + \tau_0\ddot{w}_{,z})]. \tag{17}
 \end{aligned}$$

Note that Eq. (17) reduces to the classical coupled thermoelasticity equation for heat conduction if $\tau_0=0$.

We define the following nondimensional quantities:

$$x^* = \frac{v_x}{k_x}x, \quad y^* = \frac{v_x}{k_x}y, \quad z^* = \frac{v_x}{k_x}z, \quad t^* = \frac{v_x^2}{k_x}t,$$

$$u^* = \frac{v_x^3 \rho}{k_x \beta_{xx} T_0}u, \quad v^* = \frac{v_x^3 \rho}{k_x \beta_{xx} T_0}v,$$

$$w^* = \frac{v_x^3 \rho}{k_x \beta_{xx} T_0}w, \quad T^* = \frac{T}{T_0},$$

$$c_1 = \frac{c_{12}}{c_{11}}, \quad c_2 = \frac{c_{55}}{c_{11}}, \quad c_3 = \frac{c_{22}}{c_{11}}, \quad c_4 = \frac{c_{23}}{c_{11}},$$

$$c_5 = \frac{c_{44}}{c_{11}}, \quad \delta = c_1 + c_2, \quad \bar{\beta} = \frac{\beta_{yy}}{\beta_{xx}}, \quad \bar{K} = \frac{K_{yy}}{K_{xx}},$$

$$\tau_0^* = \frac{v_x^2}{k_x} \tau_0, \quad \varepsilon = \frac{\beta_{xx}^3 T_0}{\rho^2 C_E v_x^2},$$

where $v_x = \sqrt{c_{11}/\rho}$ is the velocity of compressional waves, $k_x = K_{xx}/\rho C_E$ is the thermal diffusivity in the x direction, and ε is the thermoelastic coupling constant. Using the above nondimensional quantities, the governing equations are now written as

$$u_{,xx} + c_1 v_{,xy} + c_1 w_{,xz} + c_2(u_{,yy} + v_{,xy}) + c_2(u_{,zz} + w_{,xz}) - T_{,x} = \ddot{u}, \tag{18}$$

$$c_2(u_{,xy} + v_{,xx}) + c_1 u_{,xy} + c_3 v_{,yy} + c_4 w_{,yz} + c_5(v_{,zz} + w_{,yz}) - \bar{\beta} T_{,y} = \ddot{v}, \tag{19}$$

$$c_2(u_{,xz} + w_{,xx}) + c_5(u_{,yz} + w_{,yy}) + c_1 u_{,xz} + c_4 v_{,yz} + c_3 w_{,zz} - \bar{\beta} T_{,z} = \ddot{w}, \tag{20}$$

$$\begin{aligned}
 &T_{,xx} + \bar{K}T_{,yy} + \bar{K}T_{,zz} - (\dot{T} + \tau_0\ddot{T}) = \varepsilon[(\dot{u}_{,x} + \tau_0\ddot{u}_{,x}) \\
 &\quad + \bar{\beta}(\dot{v}_{,y} + \tau_0\ddot{v}_{,y}) + \bar{\beta}(\dot{w}_{,z} + \tau_0\ddot{w}_{,z})]. \tag{21}
 \end{aligned}$$

Generally, the coupling term ε is small for most materials.¹⁹ Table I gives numerical values of some constants for three different materials, namely, aluminium, zinc, and silicon nitride. In the following two sections, two approaches will be

introduced to solve the above exact formulation.

1. First approach

For convenience, the asterisk will be suppressed from now on. The displacement can be written in terms of three potential functions as in Buchwald²⁰ in the form

$$u = \frac{\partial \Theta}{\partial x}, \tag{22}$$

$$u = \frac{\partial \Phi}{\partial y} + \frac{\partial \Psi}{\partial z}, \tag{23}$$

$$w = \frac{\partial \Phi}{\partial z} - \frac{\partial \Psi}{\partial y}. \tag{24}$$

Eliminating the displacements from the equations of motion produces

$$\left[c_2 \frac{\partial^2}{\partial x^2} + c_5 \nabla^2 - \frac{\partial^2}{\partial t^2} \right] \nabla^2 \Psi = 0, \tag{25}$$

$$\delta \frac{\partial^2}{\partial x^2} \nabla^2 \Phi + \left[c_2 \nabla^2 + \frac{\partial^2}{\partial x^2} - \frac{\partial^2}{\partial t^2} \right] \frac{\partial^2 \Theta}{\partial x^2} - \frac{\partial^2 T}{\partial x^2} = 0, \tag{26}$$

$$\delta \frac{\partial^2}{\partial x^2} \nabla^2 \Theta + \left[c_3 \nabla^2 + c_2 \frac{\partial^2}{\partial x^2} - \frac{\partial^2}{\partial t^2} \right] \nabla^2 \Phi - \bar{\beta} \nabla^2 T = 0, \tag{27}$$

$$\begin{aligned}
 &\varepsilon \left[\frac{\partial^2}{\partial x^2} (\dot{\Theta} + \tau_0 \ddot{\Theta}) + \bar{\beta} \nabla^2 (\dot{\Phi} + \tau_0 \ddot{\Phi}) \right] - \frac{\partial^2 T}{\partial x^2} - \bar{K} \nabla^2 T \\
 &\quad + (\dot{T} + \tau_0 \ddot{T}) = 0, \tag{28}
 \end{aligned}$$

where

$$\nabla^2 = \frac{\partial^2}{\partial z^2} + \frac{\partial^2}{\partial y^2}.$$

It can be noted that the first equation is decoupled from others. Since we are interested in propagating waves in the plane of x, y , potentials and temperature are written in the form

$$\Theta = g_1(z) e^{i(kx + \xi y - \omega t)}, \tag{29}$$

$$\Phi = g_2(z) e^{i(kx + \xi y - \omega t)}, \tag{30}$$

$$T = g_3(z) e^{i(kx + \xi y - \omega t)}, \tag{31}$$

$$\Psi = g_4(z) e^{i(kx + \xi y - \omega t)}, \tag{32}$$

where k, ξ , and ω are, respectively, the nondimensional wave number in the x direction, the nondimensional wave number

in the y direction, and nondimensional frequency.

By substitution of these assumed potentials into Eq. (25), we get a second-order ordinary differential equation in $g_4(z)$ and a second-order system of differential equation in $g_1(z)$, $g_2(z)$, and $g_3(z)$. It can be shown that the solutions have the following forms:

$$g_1 = F_1\Omega_1 + G_1\Omega_2 + H_1\Omega_3, \tag{33}$$

$$g_2 = F_2\Omega_1 + G_2\Omega_2 + H_2\Omega_3, \tag{34}$$

$$g_3 = F_3\Omega_1 + G_3\Omega_2 + H_3\Omega_3, \tag{35}$$

$$g_4 = F_4\Omega_4. \tag{36}$$

Here,

$$\Omega_1 = B_{11}e^{is_1z} + B_{12}e^{is_1(H-z)}, \tag{37}$$

$$\Omega_2 = B_{21}e^{is_2z} + B_{22}e^{is_2(H-z)}, \tag{38}$$

$$\Omega_3 = B_{31}e^{is_3z} + B_{32}e^{is_3(H-z)}, \tag{39}$$

$$\Omega_4 = B_{41}e^{irz} + B_{42}e^{ir(H-z)}. \tag{40}$$

Using Eqs. (29)–(32) and the expression for $g_1(z)$, $g_2(z)$, and $g_3(z)$ in Eqs. (25)–(28), we get for nontrivial solution

$$r = \sqrt{\frac{\omega^2 - c_2k^2 - c_5\xi^2}{c_5}} \tag{41}$$

and the determinant of the following matrix must vanish,

$$\begin{bmatrix} -c_2X - k^2 + \omega^2 & -\delta X & -1 \\ -\delta k^2 & -c_3X - c_2k^2 + \omega^2 & -\bar{\beta} \\ \varepsilon\tau k^2 & \bar{\beta}\varepsilon\tau X & k^2 + \bar{K}X - \tau \end{bmatrix}, \tag{42}$$

where

$$X = (s^2 + \ell^2)$$

and

$$\tau = (i\omega + \tau_0\omega^2),$$

and s is the nondimensional wave number in the z -direction. This results in the following cubic equation:

$$X^3 + A_1X^2 + A_2X + A_3 = 0, \tag{43}$$

where A_1 , A_2 , and A_3 are defined in Appendix A. Solving Eq. (43) yields the following three roots for s^2 :

$$s_1^2 = -\xi^2 - \frac{A_1}{3} - \frac{\sqrt[3]{2}\Lambda}{3(\Upsilon + \sqrt{4\Lambda^3 + \Upsilon^2})^{1/3}} + \frac{(\Upsilon + \sqrt{4\Lambda^3 + \Upsilon^2})^{1/3}}{3\sqrt[3]{2}}, \tag{44}$$

$$s_2^2 = -\xi^2 - \frac{A_1}{3} - \frac{(1 + i\sqrt{3}\Lambda)}{3\sqrt[3]{2}(\Upsilon + \sqrt{4\Lambda^3 + \Upsilon^2})^{1/3}} - \frac{(1 - i\sqrt{3})\Lambda}{6\sqrt[3]{2}}, \tag{45}$$

$$s_3^2 = -\xi^2 - \frac{A_1}{3} - \frac{(1 - i\sqrt{3}\Lambda)}{3\sqrt[3]{2}(\Upsilon + \sqrt{4\Lambda^3 + \Upsilon^2})^{1/3}} - \frac{(1 + i\sqrt{3})\Lambda}{6\sqrt[3]{2}}, \tag{46}$$

where $\Lambda = 3A_2 - A_1^2$ and $\Upsilon = -2A_1^3 + 9A_1A_2 - 27A_3$. The constants appearing in Eqs. (33)–(36) may be taken as shown in Appendix A. Now, the temperature gradient and the stresses of interest are

$$\sigma_{zz} = \mathbf{m}_{zz}\mathbf{D}\mathbf{v}, \tag{47}$$

$$\sigma_{xz} = \mathbf{m}_{xz}\mathbf{D}\mathbf{v}, \tag{48}$$

$$\sigma_{yz} = \mathbf{m}_{yz}\mathbf{D}\mathbf{v}, \tag{49}$$

$$T_z = \mathbf{m}_T\mathbf{D}\mathbf{v}, \tag{50}$$

where the row vectors \mathbf{m}_{zz} , \mathbf{m}_{xz} , \mathbf{m}_{yz} , and \mathbf{m}_T are defined in Appendix A. The matrix \mathbf{D} is a diagonal matrix such that

$$\text{diag}[\mathbf{D}] = [e^{is_1z}, e^{is_2z}, e^{is_3z}, e^{irz}, e^{is_1(H-z)}, e^{is_2(H-z)}, e^{is_3(H-z)}, e^{ir(H-z)}] \tag{51}$$

and the generalized coefficients vector can be written as

$$\mathbf{v} = \{B_{11} B_{21} B_{31} B_{41} B_{12} B_{22} B_{32} B_{42}\}^T. \tag{52}$$

The boundary conditions are that stresses and temperature gradient on the surfaces of the plate should vanish. Hence, we demand that

$$T_{,z} = \sigma_{zz} = \sigma_{zx} = \sigma_{zy} = 0. \tag{53}$$

Using boundary conditions (53) in the resulting stresses and temperature gradient yields eight equations involving the vector \mathbf{v} . In order for the eight boundary conditions to be satisfied simultaneously, the determinant of the coefficient of the arbitrary constants in Eq. (52) must vanish. This gives an equation for the frequency of the guided wave for a given wave number.

2. Second approach

For an infinite plate one can use Fourier transformation in space and time domains represented by the following integral:

$$\hat{\Phi}(k, \xi, z; \omega) = \int_{-\infty}^{\infty} \int_{-\infty}^{\infty} \int_{-\infty}^{\infty} \Phi(x, y, z; t) e^{i(kx + \xi y - \omega t)} dx dy dt. \tag{54}$$

Here, k, ξ are the wave numbers in x and y directions, respectively, and ω the circular frequency. Applying the Fourier

transformation (54) to the governing equations will yield the following eigenvalue problem:

$$[A]S_{,z} = [B]S, \tag{55}$$

were $S_{,z} = dS/dz$ and

$$S(z) = [\hat{u} \ \hat{v} \ \hat{w} \ \hat{T} \ \hat{\sigma}_{zx} \ \hat{\sigma}_{yz} \ \hat{\sigma}_{zz} \ \hat{T}_{,z}]^T. \tag{56}$$

The general solution can be obtained by determining the eigenvalues and the eigenvectors of Eq. (55). Here S is the displacement-temperature-traction vector and matrices A and B are defined as

$$A = \begin{bmatrix} \cdot & \cdot & \cdot & -1 & \cdot & \cdot & \cdot & \cdot \\ \cdot & \cdot & -c_3 & \cdot & \cdot & \cdot & \cdot & \cdot \\ \cdot & -c_5 & \cdot & \cdot & \cdot & \cdot & \cdot & \cdot \\ -c_2 & \cdot & \cdot & \cdot & \cdot & \cdot & \cdot & \cdot \\ \cdot & \cdot & ic_1k & \cdot & 1 & \cdot & \cdot & \cdot \\ \cdot & \cdot & ic_4\xi & \cdot & \cdot & 1 & \cdot & \cdot \\ \cdot & \cdot & \cdot & \cdot & \cdot & \cdot & 1 & \cdot \\ \cdot & \cdot & \bar{\beta}\varepsilon\tau & \cdot & \cdot & \cdot & \cdot & \bar{K} \end{bmatrix}, \tag{57}$$

$$B = \begin{bmatrix} \cdot & \cdot & \cdot & \cdot & \cdot & \cdot & \cdot & -1 \\ ic_1k & \cdot & ic_4\xi & \cdot & -\bar{\beta} & \cdot & \cdot & -1 \\ \cdot & \cdot & \cdot & ic_5\xi & \cdot & \cdot & -1 & \cdot \\ \cdot & \cdot & \cdot & ic_2k & \cdot & \cdot & -1 & \cdot \\ k^2 + c_2\xi^2 - \omega^2 & k\xi(c_1 + c_2) & \cdot & ik & \cdot & \cdot & \cdot & \cdot \\ k\xi(c_1 + c_2) & c_2k^2 + c_3\xi^2 - \omega^2 & \cdot & i\bar{\beta}\xi & \cdot & \cdot & \cdot & \cdot \\ \cdot & \cdot & \cdot & -\omega^2 & \cdot & \cdot & -ik & -i\xi \\ -i\varepsilon k\tau & -i\bar{\beta}\varepsilon\tau & \cdot & k^2 + \bar{K}\xi^2 - \tau & \cdot & \cdot & \cdot & \cdot \end{bmatrix}, \tag{58}$$

where $\tau = i\omega + \tau_0\omega^2$.

The general solution to Eq. (55) can be written as

$$S(z) = [QE]\{C\}, \tag{59}$$

where Q is the resulting eigenvectors matrix from Eq. (55), C are generalized coefficients, and E is a diagonal matrix,

$$E = \text{diag}[e^{is_1z}, e^{is_2z}, e^{is_3z}, e^{is_4z}, e^{is_1(H-z)}, e^{is_2(H-z)}, e^{is_3(H-z)}, e^{is_4(H-z)}], \tag{60}$$

where $1, \dots, 4is_p, (p=1, 2, 3)$ are the resulting eigenvalues of the characteristics equations (55), with $\text{Im}(s_p) \geq 0$. The first four elements of Eq. (60) represent the wave propagation along the positive z axis, while the last four elements represent the wave propagation along the negative z axis.

The boundary conditions are that tractions and temperature gradient in the z direction on the surfaces of the plate should vanish. Applying these boundary conditions yields the dispersion relation for the infinite plate.

B. Finite element method

We rewrite the governing equations in vector form,

$$\{\sigma\} = [C]\{\varepsilon\} - \{\beta\}T, \tag{61}$$

$$\rho \dot{\eta} = \{\beta\}^T \{\dot{\varepsilon}\} + \frac{\rho C_E}{T_0} \dot{T}, \tag{62}$$

$$\{q\} + \tau_0\{\dot{q}\} = -[K]\{T'\}, \tag{63}$$

where $T' = T_j$.

The plate is divided into N parallel, homogeneous, and anisotropic layers, which are perfectly bonded together. A global rectangular coordinate system (X, Y, Z) is adopted such that X and Y axes lie in the midplane of the plate, and Z axis parallel to the thickness direction of the plate. To analyze the guided wave propagation in such an infinite plate, we discretize the thickness of the plate using three-noded bar elements, each of which has associated with it a local coordinate axes (x, y, z) , which are parallel to the global coordinate axes.

Two sets of shape functions are introduced to approximate the displacement and temperature fields on the element level,

$$\mathbf{u}(x, y, z, t) = N_1^e(z)\mathbf{u}^e(x, y, t), \tag{64}$$

$$\mathbf{T}(x, y, z, t) = N_2^e(z)\mathbf{T}^e(x, y, t), \tag{65}$$

where

$$N_1^e = \begin{bmatrix} N_1 & 0 & 0 & N_2 & 0 & 0 & N_3 & 0 & 0 \\ 0 & N_1 & 0 & 0 & N_2 & 0 & 0 & N_3 & 0 \\ 0 & 0 & N_1 & 0 & 0 & N_2 & 0 & 0 & N_3 \end{bmatrix} \tag{66}$$

and

$$N_2^T = \{N_1 N_2 N_3\}. \tag{67}$$

Nodal displacements and temperatures are stored in the two vectors \mathbf{u}^e and $\boldsymbol{\theta}^e$, respectively. Using generalized linear thermoelasticity the strain tensor and temperature vector is derived from the kinematic equations,

$$\boldsymbol{\epsilon} = \mathbf{D}_1\mathbf{u}_{,x}^e + \mathbf{D}_2\mathbf{u}_{,y}^e + \mathbf{D}_3\mathbf{u}^e, \tag{68}$$

$$\mathbf{T}' = \mathbf{B}_1\mathbf{T}_{,x}^e + \mathbf{B}_2\mathbf{T}_{,y}^e + \mathbf{B}_3\mathbf{T}^e, \tag{69}$$

where $\mathbf{B}_1, \mathbf{B}_2, \mathbf{B}_3, \mathbf{D}_1, \mathbf{D}_2$, and \mathbf{D}_3 are defined in Appendix B. The variational forms of Eqs. (68) and (69) are

$$\delta\boldsymbol{\epsilon} = \mathbf{D}_1\delta\mathbf{u}_{,x}^e + \mathbf{D}_2\delta\mathbf{u}_{,y}^e + \mathbf{D}_3\delta\mathbf{u}^e, \tag{70}$$

$$\delta\mathbf{T}' = \mathbf{B}_1\delta\mathbf{T}_{,x}^e + \mathbf{B}_2\delta\mathbf{T}_{,y}^e + \mathbf{B}_3\delta\mathbf{T}^e. \tag{71}$$

Considering the body force \mathbf{f}^e , the virtual displacement principle can be written as the following form:

$$\begin{aligned} \int_{t_0}^{t_1} \int_V [\delta\boldsymbol{\epsilon}^T\boldsymbol{\sigma} - \delta\mathbf{T}'^T\mathbf{K}\mathbf{T}' - \delta\mathbf{T}'^T(q_i + \tau_0\dot{q}_i)]dV dt \\ = \int_{t_0}^{t_1} \int_V \delta\mathbf{u}^T(\mathbf{f} - \rho\ddot{\mathbf{u}})dV dt. \end{aligned} \tag{72}$$

Substituting the constitutive relations, Eqs. (61)–(63), into the variational form, Eq. (72), leads to the following terms:

$$\begin{aligned} \int_{t_0}^{t_1} \int_V \delta\boldsymbol{\epsilon}^T\boldsymbol{\sigma}dV dt &= \int_{t_0}^{t_1} \int_V \delta\boldsymbol{\epsilon}^T(\mathbf{C}\boldsymbol{\epsilon} - \beta\mathbf{T})dV dt \\ &= \int_{t_0}^{t_1} \int_V [(\delta\mathbf{u}_{,x}^e\mathbf{D}_1^T + \delta\mathbf{u}_{,y}^e\mathbf{D}_2^T + \delta\mathbf{u}^e\mathbf{D}_3^T)\mathbf{C}(\mathbf{D}_1\delta\mathbf{u}_{,x}^e + \mathbf{D}_2\delta\mathbf{u}_{,y}^e + \mathbf{D}_3\delta\mathbf{u}^e) - (\mathbf{u}_{,x}^e\mathbf{D}_1^T + \mathbf{u}_{,y}^e\mathbf{D}_2^T \\ &\quad + \mathbf{u}^e\mathbf{D}_3^T)\beta N_2^T\mathbf{T}^e]dV dt \\ &= \int_{t_0}^{t_1} \int_y \int_x \delta\mathbf{u}^e\mathbf{T}^e[-\mathbf{k}_{11}^e\mathbf{u}_{,xx}^e - \mathbf{k}_{12}^e\mathbf{u}_{,xy}^e - \mathbf{k}_{13}^e\mathbf{u}_{,x}^e - \mathbf{k}_{21}^e\mathbf{u}_{,xy}^e - \mathbf{k}_{22}^e\mathbf{u}_{,yy}^e - \mathbf{k}_{23}^e\mathbf{u}_{,y}^e + \mathbf{k}_{31}^e\mathbf{u}_{,x}^e + \mathbf{k}_{32}^e\mathbf{u}_{,y}^e + \mathbf{k}_{33}^e\mathbf{u}_{,yy}^e \\ &\quad + \mathbf{k}_{m01}^e\mathbf{T}_{,x}^e + \mathbf{k}_{m02}^e\mathbf{T}_{,y}^e - \mathbf{k}_{m03}^e\mathbf{T}_{,x}^e]dx dy dt, \end{aligned} \tag{73}$$

where the elemental matrices appearing in the last equation are defined in Appendix B. The second term in Eq. (72) can be written as

$$\begin{aligned} \int_{t_0}^{t_1} \int_V \delta(\mathbf{T}^e\mathbf{T}')^T\mathbf{K}(\mathbf{T}^e)'dV dt \\ = \int_{t_0}^{t_1} \int_V (\delta\mathbf{T}_{,x}^e{}^T\mathbf{B}_1^T + \delta\mathbf{T}_{,y}^e\mathbf{B}_2^T + \delta\mathbf{T}^e\mathbf{B}_3^T) \\ \times \mathbf{K}(\mathbf{B}_1\mathbf{T}_{,x}^e + \mathbf{B}_2\mathbf{T}_{,y}^e + \mathbf{B}_3\mathbf{T}^e)dV dt \end{aligned}$$

$$= \int_{t_0}^{t_1} \int_y \int_x \delta\mathbf{T}^e\mathbf{T}^e(\mathbf{g}_{11}^e\mathbf{T}_{,xx}^e + \mathbf{g}_{22}^e\mathbf{T}_{,yy}^e - \mathbf{g}_{33}^e\mathbf{T}^e)dx dy dt, \tag{74}$$

where $\mathbf{g}_{11}, \mathbf{g}_{22}$, and \mathbf{g}_{33} are defined as

$$\begin{aligned} \mathbf{g}_{11}^e &= \int_z \mathbf{B}_1^T\mathbf{K}\mathbf{B}_1dz, & \mathbf{g}_{22}^e &= \int_z \mathbf{B}_2^T\mathbf{K}\mathbf{B}_2dz, \\ \mathbf{g}_{33}^e &= \int_z \mathbf{B}_3^T\mathbf{K}\mathbf{B}_3dz. \end{aligned}$$

The third term of Eq. (72) is

$$\begin{aligned}
 & \int_{t_0}^{t_1} \int_V \delta(\mathbf{T}^{eT})'(\mathbf{q} + \tau_0 \dot{\mathbf{q}}) dV dt \\
 &= - \int_{t_0}^{t_1} \int_V \delta \mathbf{T}^{eT}(\mathbf{q}' + \tau_0 \dot{\mathbf{q}}') dV dt \\
 &= \int_{t_0}^{t_1} \int_V \delta \mathbf{T}^{eT}(T_0 \rho \dot{\eta} + \tau_0 T_0 \rho \dot{\eta}) dV dt \\
 &= \int_{t_0}^{t_1} \int_y \int_x \delta \mathbf{T}^{eT}[(\mathbf{f}_1^e \dot{\mathbf{u}}_{,x}^e + \mathbf{f}_2^e \dot{\mathbf{u}}_{,y}^e + \mathbf{f}_3^e \dot{\mathbf{u}}^e + \mathbf{m}_{\theta\theta}^e \dot{\mathbf{T}}) \\
 & \quad + \tau_0(\mathbf{f}_1 \dot{\mathbf{u}}_{,x}^e + \mathbf{f}_2 \dot{\mathbf{u}}_{,y}^e + \mathbf{f}_3 \dot{\mathbf{u}}^e + \mathbf{m}_{\theta\theta}^e \dot{\mathbf{T}})] dx dy dt, \tag{75}
 \end{aligned}$$

where $\mathbf{q}' = \mathbf{q}_{,i}$ and

$$\begin{aligned}
 \mathbf{m}_{\theta\theta}^e &= \int_z N_2^e \rho N_2^{eT} dz, \quad \mathbf{f}_1^e = \int_z T_0 N_2^e \beta \mathbf{D}_1 dz, \\
 \mathbf{f}_2^e &= \int_z T_0 N_2^e \beta \mathbf{D}_2 dz, \quad \mathbf{f}_3^e = \int_z T_0 N_2^e \beta \mathbf{D}_3 dz
 \end{aligned}$$

The right-hand side of Eq. (72) is written as

$$\begin{aligned}
 & \int_{t_0}^{t_1} \int_V \delta \mathbf{u}^T(\mathbf{f} - \rho \ddot{\mathbf{u}}) dV dt \\
 &= \int_{t_0}^{t_1} \int_V \delta \mathbf{u}^T N_1^{eT}(\mathbf{f} - \rho N_1^e \ddot{\mathbf{u}}^e) dV dt \\
 &= \int_{t_0}^{t_1} \int_y \int_x \delta \mathbf{u}^T(\mathbf{f}^e - \mathbf{m}^e \ddot{\mathbf{u}}^e) dx dy dt, \tag{76}
 \end{aligned}$$

where

$$\mathbf{f}^e = \int_z N_1^{eT} \mathbf{f} dz, \quad \mathbf{m} = \int_z \rho N_1^e N_1^{eT} dz.$$

Equating the coefficient of δu^e in Eq. (72) to zero yields

$$\begin{aligned}
 & \mathbf{k}_{11}^e \mathbf{u}_{,xx}^e + \mathbf{k}_{12}^e \mathbf{u}_{,xy}^e + \mathbf{k}_{13}^e \mathbf{u}_{,x}^e + \mathbf{k}_{21}^e \mathbf{u}_{,xy}^e + \mathbf{k}_{22}^e \mathbf{u}_{,yy}^e + \mathbf{k}_{23}^e \mathbf{u}_{,y}^e \\
 & \quad - \mathbf{k}_{31}^e \mathbf{u}_{,x}^e - \mathbf{k}_{32}^e \mathbf{u}_{,y}^e - \mathbf{k}_{33}^e \mathbf{u}^e - \mathbf{k}_{m01}^e \mathbf{T}_{,x}^e - \mathbf{k}_{m02}^e \mathbf{T}_{,y}^e + \mathbf{k}_{m03}^e \mathbf{T}^e \\
 & \quad - \mathbf{m}^e \ddot{\mathbf{u}}^e = 0. \tag{77}
 \end{aligned}$$

Similarly, equating the coefficient of $\delta \mathbf{T}^e$ in Eq. (72) yields

$$\begin{aligned}
 & \tau_0 \mathbf{m}_{\theta\theta}^e \dot{\mathbf{T}}^e + \mathbf{m}_{\theta\theta}^e \dot{\mathbf{T}}^e + \tau_0 \mathbf{f}_1^e \dot{\mathbf{u}}_{,x}^e + \tau_0 \mathbf{f}_2^e \dot{\mathbf{u}}_{,y}^e + \tau_0 \mathbf{f}_3^e \dot{\mathbf{u}}^e + \mathbf{f}_1^e \dot{\mathbf{u}}_{,x}^e \\
 & \quad + \mathbf{f}_2^e \dot{\mathbf{u}}_{,y}^e + \mathbf{f}_3^e \dot{\mathbf{u}}^e - \mathbf{g}_{11}^e \mathbf{T}_{,xx}^e - \mathbf{g}_{22}^e \mathbf{T}_{,yy}^e + \mathbf{g}_{33}^e \mathbf{T}^e = 0. \tag{78}
 \end{aligned}$$

Rewriting the last two equations [Eqs. (77) and (78)] in vector formats yields

$$\begin{aligned}
 & [-\mathbf{M} : 0] \begin{Bmatrix} \ddot{\mathbf{u}}^e \\ \cdots \\ \dot{\mathbf{T}}^e \end{Bmatrix} + [\mathbf{K}_{11} : 0] \begin{Bmatrix} \mathbf{u}_{,xx}^e \\ \cdots \\ \mathbf{T}_{,xx}^e \end{Bmatrix} + [\mathbf{K}_{12} + \mathbf{K}_{21} : 0] \begin{Bmatrix} \mathbf{u}_{,xy}^e \\ \cdots \\ \mathbf{T}_{,xy}^e \end{Bmatrix} \\
 & \quad + [\mathbf{K}_{13} - \mathbf{K}_{31} : -\mathbf{K}_{m01}] \begin{Bmatrix} \mathbf{u}_{,x}^e \\ \cdots \\ \mathbf{T}_{,x}^e \end{Bmatrix} + [\mathbf{K}_{22} : 0] \begin{Bmatrix} \mathbf{u}_{,yy}^e \\ \cdots \\ \mathbf{T}_{,yy}^e \end{Bmatrix} \\
 & \quad + [\mathbf{K}_{23} - \mathbf{K}_{32} : -\mathbf{K}_{m02}] \begin{Bmatrix} \mathbf{u}_{,y}^e \\ \cdots \\ \mathbf{T}_{,y}^e \end{Bmatrix} + [-\mathbf{K}_{33} : \mathbf{K}_{m03}] \begin{Bmatrix} \mathbf{u}^e \\ \cdots \\ \mathbf{T}^e \end{Bmatrix} = 0. \tag{79}
 \end{aligned}$$

and

$$\begin{aligned}
 & [\tau_0 \mathbf{F}_3 : \tau_0 \mathbf{F}_{\theta\theta}] \begin{Bmatrix} \ddot{\mathbf{u}}^e \\ \cdots \\ \dot{\mathbf{T}}^e \end{Bmatrix} + [\tau_0 \mathbf{F}_1 : 0] \begin{Bmatrix} \ddot{\mathbf{u}}_{,x}^e \\ \cdots \\ \dot{\mathbf{T}}_{,x}^e \end{Bmatrix} + [\tau_0 \mathbf{F}_2 : 0] \begin{Bmatrix} \ddot{\mathbf{u}}_{,y}^e \\ \cdots \\ \dot{\mathbf{T}}_{,y}^e \end{Bmatrix} \\
 & \quad + [\mathbf{F}_1 : 0] \begin{Bmatrix} \dot{\mathbf{u}}_{,x}^e \\ \cdots \\ \dot{\mathbf{T}}_{,x}^e \end{Bmatrix} + [\mathbf{F}_2 : 0] \begin{Bmatrix} \dot{\mathbf{u}}_{,y}^e \\ \cdots \\ \dot{\mathbf{T}}_{,y}^e \end{Bmatrix} + [\mathbf{F}_3 : \mathbf{M}_{\theta\theta}] \begin{Bmatrix} \dot{\mathbf{u}}^e \\ \cdots \\ \dot{\mathbf{T}}^e \end{Bmatrix} \\
 & \quad + [0 : -\mathbf{G}_{11}] \begin{Bmatrix} \mathbf{u}_{,xx}^e \\ \cdots \\ \mathbf{T}_{,xx}^e \end{Bmatrix} + [0 : -\mathbf{G}_{22}] \begin{Bmatrix} \mathbf{u}_{,yy}^e \\ \cdots \\ \mathbf{T}_{,yy}^e \end{Bmatrix} + [0 : -\mathbf{G}_{33}] \\
 & \quad \times \begin{Bmatrix} \mathbf{u}^e \\ \cdots \\ \mathbf{T}^e \end{Bmatrix} = 0. \tag{80}
 \end{aligned}$$

We assemble the element matrices into the global matrices in the standard manner to yield the equations of motion,

$$\begin{aligned}
 & \mathbf{H}_1 \ddot{\mathbf{V}} + \mathbf{H}_2 \ddot{\mathbf{V}}_{,x} + \mathbf{H}_3 \ddot{\mathbf{V}}_{,y} + \mathbf{H}_4 \dot{\mathbf{V}}_{,x} + \mathbf{H}_5 \dot{\mathbf{V}}_{,y} + \mathbf{H}_6 \dot{\mathbf{V}} + \mathbf{H}_7 \mathbf{V}_{,xx} \\
 & \quad + \mathbf{H}_8 \mathbf{V}_{,xy} + \mathbf{H}_9 \mathbf{V}_{,yy} + \mathbf{H}_{10} \mathbf{V}_{,x} + \mathbf{H}_{11} \mathbf{V}_{,y} + \mathbf{H}_{12} \mathbf{V} = \mathbf{0}, \tag{81}
 \end{aligned}$$

where the matrices \mathbf{H}_i are defined in Appendix B and \mathbf{V} is the column vector of assembled nodal displacements and temperatures.

For a wave propagating in the XY plane, we take the Fourier transform of $\mathbf{V}(X, Y, t)$ as

$$\hat{\mathbf{V}}(k_x, k_y, \omega) = \int_{-\infty}^{\infty} \int_{-\infty}^{\infty} \int_{-\infty}^{\infty} \mathbf{V}(X, Y, t) e^{i(k_x X + k_y Y - \omega t)} dX dY dt. \tag{82}$$

Applying the Fourier transform to Eq. (81) leads to the following expression:

$$\begin{aligned}
 & [\omega^2 \mathbf{H}_1 + i\omega^2 k_x \mathbf{H}_2 + i\omega^2 k_y \mathbf{H}_3 - \omega k_x \mathbf{H}_4 - \omega k_y \mathbf{H}_5 + i\omega \mathbf{H}_6 \\
 & \quad + k_x^2 \mathbf{H}_7 + k_x k_y \mathbf{H}_8 + k_y^2 \mathbf{H}_9 - i k_x \mathbf{H}_{10} - i k_y \mathbf{H}_{11} - \mathbf{H}_{12}] \hat{\mathbf{V}} = \mathbf{0}, \tag{83}
 \end{aligned}$$

where ω is the circular frequency and k_x and k_y are the wave numbers in the X and Y directions. For wave propagating in arbitrary direction in the xy plane making an angle θ with X

TABLE II. Physical data for Si₃N₄.

Quantity	Units	Numerical value
ρ	kg/m ³	3.20×10^3
c_{11}	N/m ²	5.74×10^{11}
c_{12}	N/m ²	1.27×10^{11}
c_{22}	N/m ²	4.33×10^{11}
c_{23}	N/m ²	1.95×10^{11}
c_{55}	N/m ²	1.08×10^{11}
T_0	K	296
β_{xx}	N/m ² K	3.22×10^6
β_{yy}	N/m ² K	2.71×10^6
C_E	J/kg K	0.67×10^3
K_{xx}	W/m K	55.4
K_{yy}	W/m K	43.5
ε	...	2.49×10^{-3}

axis i.e., $k_x = k \cos \theta$, and $k_y = k \sin \theta$, Eq. (83) is written as

$$(k^2 \bar{\mathbf{M}} + k \bar{\mathbf{C}} + \bar{\mathbf{K}}) \hat{\mathbf{V}} = 0, \tag{84}$$

where k is the wave number of the wave in the propagation direction, and

$$\bar{\mathbf{M}} = -\cos^2 \theta \mathbf{H}_7 - \cos \theta \sin \theta \mathbf{H}_8 - \sin^2 \theta \mathbf{H}_9, \tag{85}$$

$$\begin{aligned} \bar{\mathbf{C}} = & -i\omega^2 \cos \theta \mathbf{H}_2 - i\omega^2 \sin \theta \mathbf{H}_3 + \omega \cos \theta \mathbf{H}_4 \\ & + \omega \sin \theta \mathbf{H}_5 + i \cos \theta \mathbf{H}_{10} + i \sin \theta \mathbf{H}_{11}, \end{aligned} \tag{86}$$

$$\bar{\mathbf{K}} = -\omega^2 \mathbf{H}_1 - i\omega \mathbf{H}_6 + \mathbf{H}_{12}. \tag{87}$$

Solving the eigenvalue problem represented by Eq. (84) will determine the dispersion for guided thermoelastic waves in infinite plates.

III. RESULTS AND DISCUSSION

With the view of illustrating the numerical results obtained by methods presented in the preceding sections, the material chosen for the plate is silicon nitride (Si₃N₄), the physical data for which is given in Table II. Elastic stiffness constants can be found in Ref. 21, whereas thermal properties are collected from Swift *et al.*,²² Kitayama *et al.*,²³ and Yakota and Ibukiyama.²⁴

The dimensional speed of the thermal wave in the x direction for unbounded medium is

$$v_t = \sqrt{\frac{K_{xx}}{\rho C_E \tau_0}}. \tag{88}$$

We recall that the relaxation time τ_0 is introduced to account for the finite speed of thermal wave. To the best of our knowledge, no experimental values for τ_0 have been reported. However, some researchers suggested different ways of calculating it. Chester²⁵ approximates the speed of the thermal wave according to the following equation:

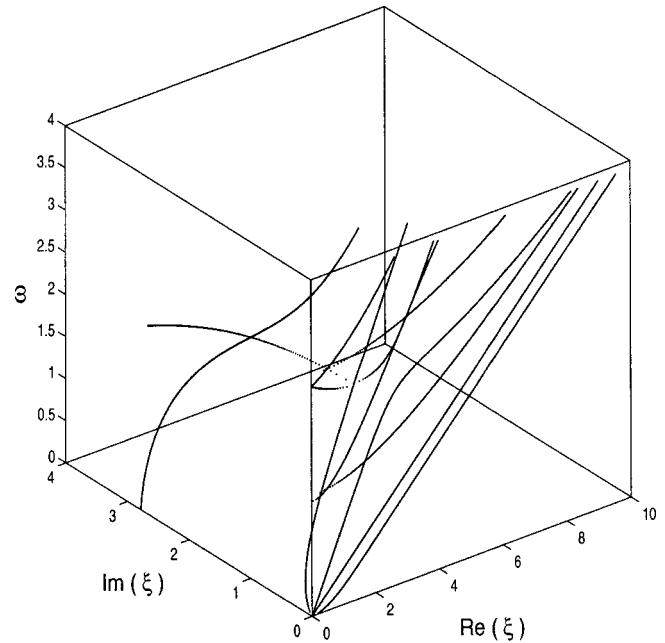


FIG. 2. 3D frequency spectrum, $\tau_0 = 1.0$.

$$v_t = \frac{v_x}{\sqrt{3}}. \tag{89}$$

Using this approximation, the dimensional relaxation time is obtained as

$$\tau_0 = \frac{3K_{xx}}{C_E C_{11}}. \tag{90}$$

Hence, for silicon nitride, τ_0 is approximately 4.322×10^{-13} s (τ_0 -nondim=3.0). Prevost and Tao²⁶ and Khadrawi, Al-Nimr, and Hammad²⁷ approximated the relaxation time by restricting the speed of the thermal wave to be

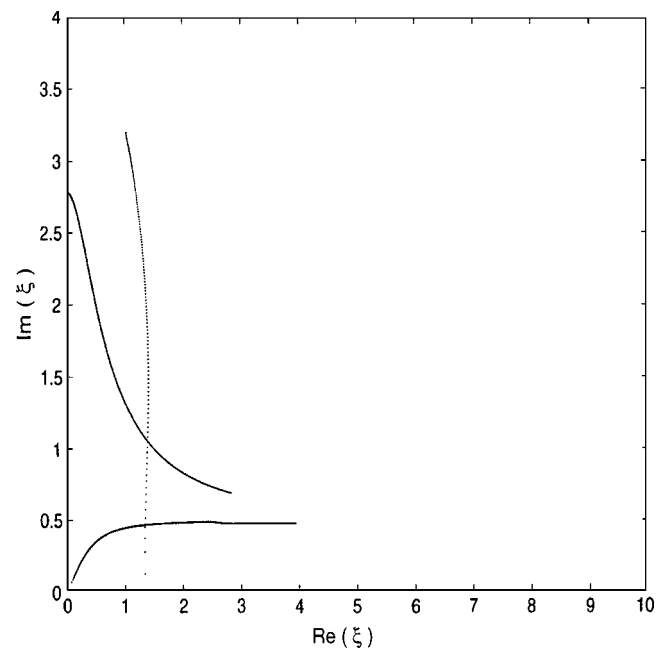


FIG. 3. Top view of frequency spectrum.

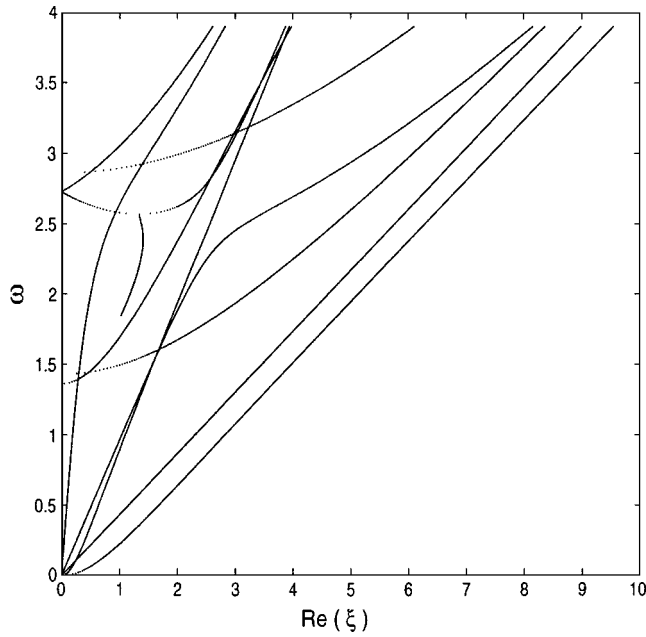


FIG. 4. Front view of the spectrum.

equal to the speed of the longitudinal wave giving the following formula for the relaxation time:

$$\tau_0 = \frac{K_{xx}}{C_E C_{11}} \tag{91}$$

This gives a value τ_0 to be 1.440×10^{-13} s (τ_0 -nondim = 1.0) for silicon nitride. The two cases will be considered in our analysis.

Numerical results are presented in the form of three-dimensional view of frequency spectrum. These are obtained by keeping ω real and letting k to be complex. Then, the phase velocity is defined as $c = \omega / \text{Re}(k)$, and the imaginary part of the k is a measure of the attenuation of the wave in

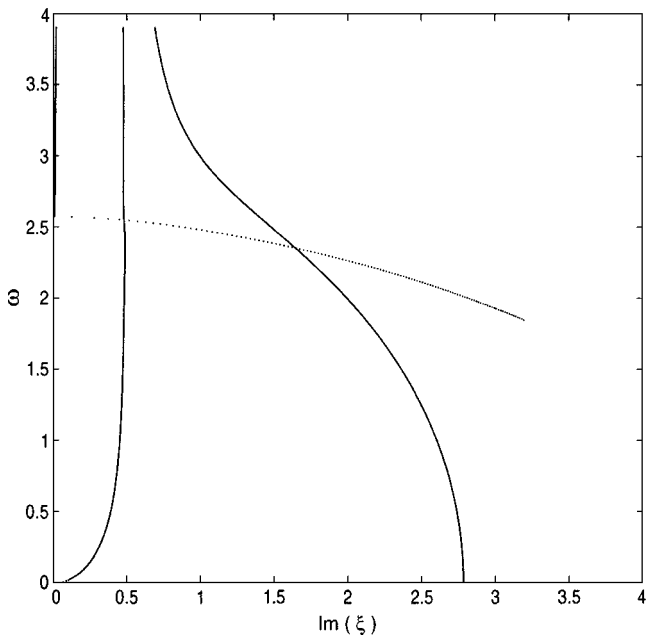


FIG. 5. Right view of the spectrum.

TABLE III. Representative values of k at $\omega=3.00$, with $\tau_0=3.0$.

Re(ξ)	Im(ξ)
7.4603	3.7701×10^{-5}
6.9277	0
6.0917	0
3.0555	0.4783
2.8532	0.0146
2.8093	0.0013
2.1112	0
1.5155	0.9932
0.8800	3.5483×10^{-4}

space. In order to find the solutions of the characteristic equation (53) of the exact analysis, Muller’s method is used to solve it as an analytic complex function. The relations between the frequency and the wave number expressed by the characteristic equation yield an infinite number of branches for an infinite number of elastic and thermal modes. The dispersion curves of first few modes have been computed and represented graphically in Figs. 2–5 for wave propagation along the x axis, i.e., $\theta=0$. The first figure shows a 3D view of the frequency spectrum, respectively. Elastic modes resemble those of isothermal case since the coupling parameter ε for Si_3N_4 is quite small. Similar to the isothermal case, a complex branch is seen (Fig. 4) originating from the minimum point on the second longitudinal mode. Moreover, note that 0th-order elastic modes propagate at all frequencies, but the higher order modes have cutoff frequencies below which they are evanescent. Since the propagation direction is along a principle direction, it is seen that the horizontal shear (SH) modes are uncoupled from the other two modes. This is evidenced by the intersection of the SH wave curves with those for the S and A waves.

The first thermal mode shows a similar behavior as the lowest elastic modes; however, it shows very high attenua-

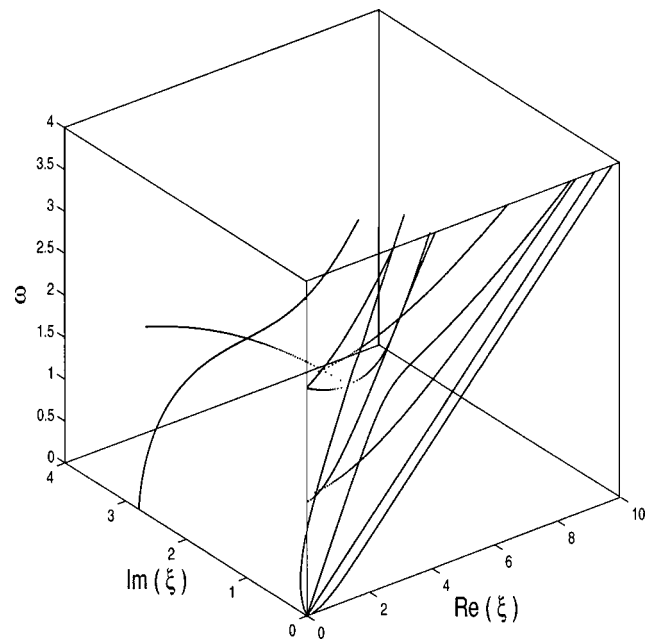


FIG. 6. Frequency spectrum using SAFE.

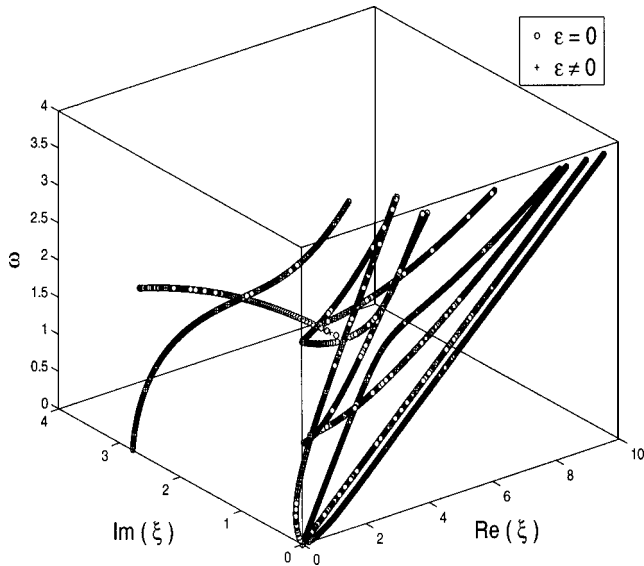


FIG. 7. Coupling effect on frequency spectrum.

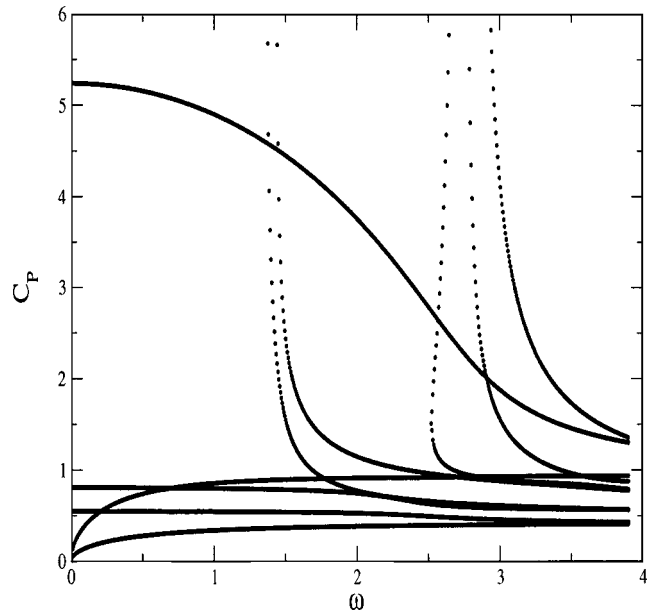


FIG. 9. Dispersion curves along $\theta=45^\circ$.

tion compared to elastic modes. Other thermal modes originate with higher imaginary values of wave numbers and eventually approach the first thermal mode. In order to see the attenuation associated with thermal modes and some elastic modes, we pick some numerical values from the frequency spectrum as shown in Table III. It is observed that some elastic modes exhibit attenuation expressed by the imaginary value of wave numbers. Points where the imaginary values are relatively high correspond to thermal modes.

Frequency spectrum was also computed by the SAFE method and graphically shown in Fig. 6. Excellent agreement between SAFE and analytic solution results is observed by comparing Fig. 6 with Fig. 2. Convergent results of SAFE analysis can be attained by relatively small number of elements (ten elements) indicating that the FEM is a powerful

and efficient technique for analyzing thermoelastic problems. Another advantage is the ease with which layered plates can be considered.

In order to see the effect of the coupling term in the heat equation, the frequency spectrum was computed for two cases, namely, $\epsilon=0$ and $\epsilon=2.94 \times 10^{-3}$. The corresponding frequency spectra are plotted in Fig. 7. The figure shows that the two spectra are undistinguishable, therefore the coupling term may be neglected without affecting the results. Doing so simplifies the exact analysis considerably because the heat equation gets decoupled from the other elastic equations. Hence Eq. (43) becomes now quadratic instead of cubic.

In Figs. 8–10 dispersion curves (normalized phase velocity vs normalized frequency) were computed and plotted along different propagation directions, namely, 0° , 45° , and

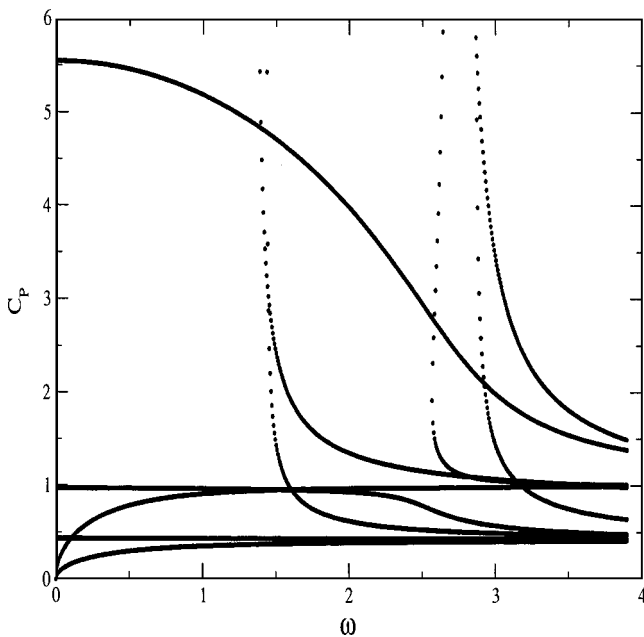


FIG. 8. Dispersion curves along $\theta=0^\circ$.

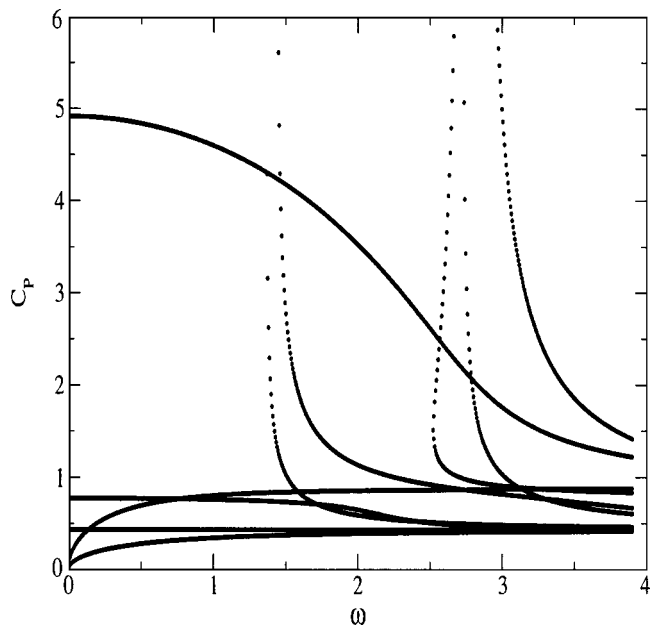


FIG. 10. Dispersion curves along $\theta=90^\circ$.

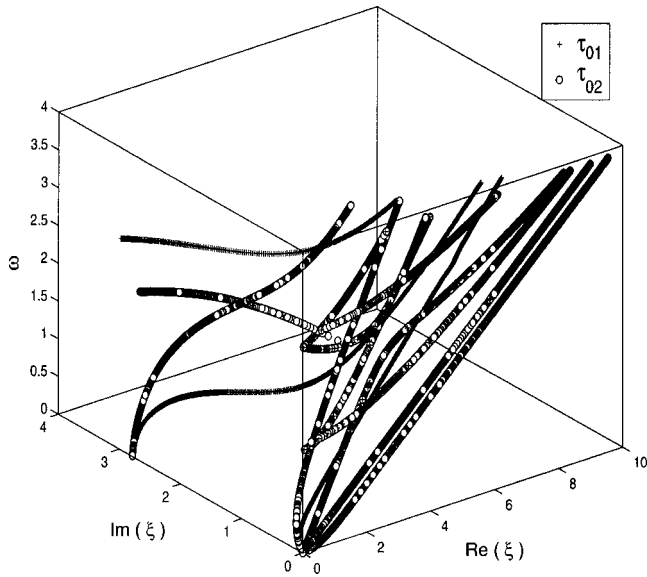


FIG. 11. The effect of relaxation time, $\tau_{01}=3.0$, $\tau_{02}=1.0$.

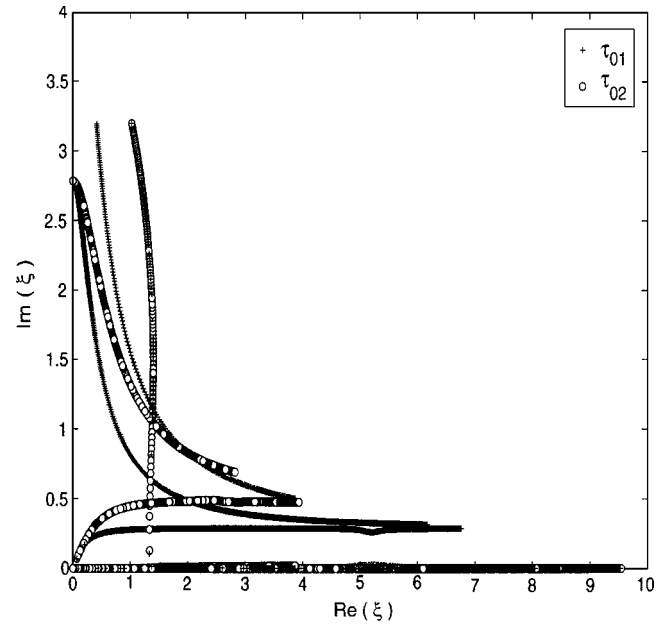


FIG. 12. Top view of Fig. 11.

90°. The figures show the effect of anisotropy of the plate on dispersion curves. For instance, the phase velocities of the elastic and thermal modes decrease as the wave travels from 0° to 90° direction. For all directions, it is seen that all thermal modes except the lowest one start with a finite phase speed and eventually approach the speed of the first thermal mode, which originates with vanishing phase speed.

Finally, the effect of relaxation time on frequency spectrum is investigated. Frequency spectrum was computed for the two values of relaxation times that resulted from using the two different formulas Eqs. (90) and (91). Figures 11 and 12 show frequency spectra for the thermoelastic plate for the two relaxation times. By examining the figure, it is noticed that influence of changing relaxation time was mainly on thermal modes. Increasing the relaxation time causes thermal modes to have more attenuation. Besides, it results in fast convergence of higher thermal modes toward the lowest one. As expected, the velocity of thermal modes increases as the relaxation time decreases.

IV. CONCLUSIONS

Propagation of guided thermoelastic waves in a homogeneous, transversely isotropic, thermally conducting plate was investigated within the framework of the generalized theory of thermoelasticity proposed by Lord and Shulman. This theory includes a thermal relaxation time in the heat conduction equation in order to model the finite speed of the thermal wave. Three different methods were used to model the guided wave dispersion. These include an exact analysis

incorporating two different solution approaches and a SAFE method. The results obtained by these methods were found to agree very well.

The results show that both elastic and thermal modes are attenuated, the thermal modes exhibit much larger attenuation than the elastic modes. The attenuation of the former is quite small. The results agree with previous observations by Hawwa and Nayfeh.²⁸

The coupling term is generally small for all materials and can be neglected. Neglecting the coupling term simplifies the analysis without noticeable effect on the frequency spectrum as we saw earlier.

Because of the small relaxation time exhibited by the materials under consideration the thermal wave modes have much larger phase speeds than the elastic modes. The effect of increasing the relaxation time is to lower the speeds of the thermal modes.

The effect of anisotropy of the material is quite pronounced on waves propagating in different directions along the plate. Thus, it is important to consider the anisotropy of the material in order to accurately model the propagation characteristics for material characterization and transient response.

While this paper dealt with the modal dispersion of guided waves, the transient response of a plate due to a laser pulse will be reported in a subsequent paper. The latter is investigated by using the modal sum and a fast Fourier transform.

APPENDIX A: EXACT ANALYSIS

$$A_1 = \frac{1}{c_2 c_3 \bar{K}} [(c_2 c_3 + c_2^2 \bar{K} + c_3 \bar{K} - \delta^2 \bar{K}) k^2 - (c_2 c_3 + c_2 \bar{\beta} \epsilon) \tau - (c_2 + c_3) \bar{K} \omega^2],$$

$$A_2 = \frac{1}{c_2 c_3 \bar{K}} [(c_2^2 + c_3 + c_2 \bar{K} - \delta^2) k^4 + (\delta^2 + 2\bar{\beta} \delta \varepsilon - c_2^2 - c_3 - c_3 \varepsilon + \bar{\beta}^2 \varepsilon) \tau k^2 - (c_2 + c_3 + \bar{K} - c_2 \bar{K}) k^2 \omega^2 + (c_2 + c_3 + \bar{\beta}^2 \varepsilon) \tau \omega^2 + \bar{K} \omega^4],$$

$$A_3 = \frac{1}{c_2 c_3 \bar{K}} [(c_2 k^6 - (1 - \varepsilon) c_2 \tau k^4 - (1 - c_2) k^4 \omega^2 + (1 + c_2 + \varepsilon) \tau k^2 \omega^2 + (k^2 - \tau) \omega^4],$$

$$F_1 = G_1 = H_1 = F_4 = 1,$$

$$F_2 = \frac{(\delta - \bar{\beta}) k^2 + \bar{\beta} [\omega^2 - c_2 (s_1^2 + \xi^2)]}{\omega^2 - c_2 k^2 - (c_3 - \bar{\beta} \delta) (s_1^2 + \xi^2)},$$

$$F_3 = \frac{[k^2 + c_2 (s_1^2 + \xi^2) - \omega^2] [c_2 k^2 + c_3 (s_1^2 + \xi^2 - \omega^2)] - \delta^2 k^2 (s_1^2 + \xi^2)}{\omega^2 - c_2 k^2 - (c_3 - \bar{\beta} \delta) (s_2^2 + \xi^2)},$$

$$G_2 = \frac{(\delta - \bar{\beta}) k^2 + \bar{\beta} [\omega^2 - c_2 (s_2^2 + \xi^2)]}{\omega^2 - c_2 k^2 - (c_3 - \bar{\beta} \delta) (s_2^2 + \xi^2)},$$

$$G_3 = \frac{[k^2 + c_2 (s_2^2 + \xi^2) - \omega^2] [c_2 k^2 + c_3 (s_2^2 + \xi^2 - \omega^2)] - \delta^2 k^2 (s_2^2 + \xi^2)}{\omega^2 - c_2 k^2 - (c_3 - \bar{\beta} \delta) (s_2^2 + \xi^2)},$$

$$H_2 = \frac{(\delta - \bar{\beta}) k^2 + \bar{\beta} [\omega^2 - c_2 (s_3^2 + \xi^2)]}{\omega^2 - c_2 k^2 - (c_3 - \bar{\beta} \delta) (s_3^2 + \xi^2)}$$

$$G_3 = \frac{[k^2 + c_2 (s_3^2 + \xi^2) - \omega^2] [c_2 k^2 + c_3 (s_3^2 + \xi^2 - \omega^2)] - \delta^2 k^2 (s_3^2 + \xi^2)}{\omega^2 - c_2 k^2 - (c_3 - \bar{\beta} \delta) (s_3^2 + \xi^2)},$$

$$\mathbf{m}_{zz} = \begin{pmatrix} -c_1 k^2 F_1 - (c_3 s_1^2 + c_4 \xi^2) F_2 - \bar{\beta} F_3 \\ -c_1 k^2 G_1 - (c_3 s_2^2 + c_4 \xi^2) G_2 - \bar{\beta} G_3 \\ -c_1 k^2 H_1 - (c_3 s_3^2 + c_4 \xi^2) H_2 - \bar{\beta} H_3 \\ c_3 r \xi F_4 - c_4 \gamma \xi F_4 \\ -c_1 k^2 F_1 - (c_3 s_1^2 + c_4 \xi^2) F_2 - \bar{\beta} F_3 \\ -c_1 k^2 G_1 - (c_3 s_2^2 + c_4 \xi^2) G_2 - \bar{\beta} G_3 \\ -c_1 k^2 H_1 - (c_3 s_3^2 + c_4 \xi^2) H_2 - \bar{\beta} H_3 \\ c_3 r \xi F_4 - c_4 \gamma \xi F_4 \end{pmatrix}^T,$$

$$\mathbf{m}_{zx} = c_2 \{-k s_1 (F_1 + F_2), -k s_2 (G_1 + G_2), -k s_3 (H_1 + H_2), k \xi F_4, k s_1 (F_1 + F_2), k s_2 (G_1 + G_2), k s_3 (H_1 + H_2), -k \xi F_4\},$$

$$\mathbf{m}_{zy} = c_5 \{-2 s_1 \xi F_2, -2 s_2 \xi G_2, -2 s_3 \xi H_2, (\xi^2 - r^2) F_4, 2 s_1 \xi F_2, 2 s_2 \xi G_2, 2 s_3 \xi H_2, -(\xi^2 - r^2) F_4\},$$

$$\mathbf{m}_T = \{i s_1 F_3, i s_2 G_3, i s_3 H_3, 0, -i s_1 F_3, -i s_2 G_3, -i s_3 H_3, 0\}.$$

APPENDIX B: FINITE ELEMENT MATRICES

$$\mathbf{B}_1 = \begin{bmatrix} N_1 & N_2 & N_3 \\ \cdot & \cdot & \cdot \\ \cdot & \cdot & \cdot \end{bmatrix}, \quad \mathbf{B}_2 = \begin{bmatrix} \cdot & \cdot & \cdot \\ N_1 & N_2 & N_3 \\ \cdot & \cdot & \cdot \end{bmatrix}, \quad \mathbf{B}_3 = \begin{bmatrix} \cdot & \cdot & \cdot \\ \cdot & \cdot & \cdot \\ N_{1,z} & N_{2,z} & N_{3,z} \end{bmatrix},$$

$$\mathbf{D}_1 = \begin{bmatrix} N_1 & \cdot & \cdot & N_2 & \cdot & \cdot & N_3 & \cdot & \cdot \\ \cdot & \cdot & \cdot & \cdot & \cdot & \cdot & \cdot & \cdot & \cdot \\ \cdot & \cdot & \cdot & \cdot & \cdot & \cdot & \cdot & \cdot & \cdot \\ \cdot & \cdot & \cdot & \cdot & \cdot & \cdot & \cdot & \cdot & \cdot \\ \cdot & \cdot & N_1 & \cdot & \cdot & N_2 & \cdot & \cdot & N_3 \\ \cdot & N_1 & \cdot & \cdot & N_2 & \cdot & \cdot & N_3 & \cdot \end{bmatrix}, \quad \mathbf{D}_2 = \begin{bmatrix} \cdot & \cdot & \cdot & \cdot & \cdot & \cdot & \cdot & \cdot & \cdot \\ \cdot & N_1 & \cdot & \cdot & N_2 & \cdot & \cdot & N_3 & \cdot \\ \cdot & \cdot & \cdot & \cdot & \cdot & \cdot & \cdot & \cdot & \cdot \\ \cdot & \cdot & \cdot & \cdot & \cdot & \cdot & \cdot & \cdot & \cdot \\ \cdot & \cdot & N_1 & \cdot & \cdot & N_2 & \cdot & \cdot & N_3 \\ N_1 & \cdot & \cdot & N_2 & \cdot & \cdot & N_3 & \cdot & \cdot \end{bmatrix},$$

$$\mathbf{D}_3 = \begin{bmatrix} \cdot & \cdot & \cdot & \cdot & \cdot & \cdot & \cdot & \cdot & \cdot \\ \cdot & \cdot & \cdot & \cdot & \cdot & \cdot & \cdot & \cdot & \cdot \\ \cdot & \cdot & N_{1,z} & \cdot & \cdot & N_{2,z} & \cdot & \cdot & N_{3,z} \\ \cdot & N_{1,z} & \cdot & \cdot & N_{2,z} & \cdot & \cdot & N_{3,z} & \cdot \\ N_{1,z} & \cdot & \cdot & N_{2,z} & \cdot & \cdot & N_{3,z} & \cdot & \cdot \end{bmatrix},$$

$$\mathbf{k}_{11}^e = \int_z \mathbf{D}_1^T \mathbf{C} \mathbf{D}_1 dz, \quad \mathbf{k}_{12}^e = \int_z \mathbf{D}_1^T \mathbf{C} \mathbf{D}_2 dz,$$

$$\mathbf{k}_{13}^e = \int_z \mathbf{D}_1^T \mathbf{C} \mathbf{D}_3 dz, \quad \mathbf{k}_{21}^e = \int_z \mathbf{D}_2^T \mathbf{C} \mathbf{D}_1 dz,$$

$$\mathbf{k}_{22}^e = \int_z \mathbf{D}_2^T \mathbf{C} \mathbf{D}_2 dz, \quad \mathbf{k}_{23}^e = \int_z \mathbf{D}_2^T \mathbf{C} \mathbf{D}_3 dz,$$

$$\mathbf{k}_{31}^e = \int_z \mathbf{D}_3^T \mathbf{C} \mathbf{D}_1 dz, \quad \mathbf{k}_{32}^e = \int_z \mathbf{D}_3^T \mathbf{C} \mathbf{D}_2 dz,$$

$$\mathbf{k}_{33}^e = \int_z \mathbf{D}_3^T \mathbf{C} \mathbf{D}_3 dz, \quad \mathbf{k}_{m01}^e = \int_z \mathbf{D}_1^T \mathbf{C} \beta N_2^{eT} dz,$$

$$\mathbf{k}_{m02}^e = \int_z \mathbf{D}_2^T \mathbf{C} \beta N_2^{eT} dz, \quad \mathbf{k}_{m03}^e = \int_z \mathbf{D}_3^T \mathbf{C} \beta N_2^{eT} dz,$$

$$\mathbf{H}_1 = \begin{bmatrix} -\mathbf{M} & \vdots & 0 \\ \dots & \dots & \dots \\ \tau_0 \mathbf{F}_3 & \vdots & \tau_0 \mathbf{M}_{\theta\theta} \end{bmatrix}, \quad \mathbf{H}_2 = \begin{bmatrix} 0 & \vdots & 0 \\ \dots & \dots & \dots \\ \tau_0 \mathbf{F}_1 & \vdots & 0 \end{bmatrix},$$

$$\mathbf{H}_3 = \begin{bmatrix} 0 & \vdots & 0 \\ \dots & \dots & \dots \\ \tau_0 \mathbf{F}_2 & \vdots & 0 \end{bmatrix}, \quad \mathbf{H}_4 = \begin{bmatrix} 0 & \vdots & 0 \\ \dots & \dots & \dots \\ \mathbf{F}_1 & \vdots & 0 \end{bmatrix},$$

$$\mathbf{H}_5 = \begin{bmatrix} 0 & \vdots & 0 \\ \dots & \dots & \dots \\ \mathbf{F}_2 & \vdots & 0 \end{bmatrix}, \quad \mathbf{H}_6 = \begin{bmatrix} 0 & \vdots & 0 \\ \dots & \dots & \dots \\ \mathbf{F}_3 & \vdots & \mathbf{M}_{\theta\theta} \end{bmatrix},$$

$$\mathbf{H}_7 = \begin{bmatrix} \mathbf{K}_{11} & \vdots & 0 \\ \dots & \dots & \dots \\ 0 & \vdots & -\mathbf{G}_{11} \end{bmatrix}, \quad \mathbf{H}_8 = \begin{bmatrix} \mathbf{K}_{12} + \mathbf{K}_{21} & \vdots & 0 \\ \dots & \dots & \dots \\ 0 & \vdots & 0 \end{bmatrix},$$

$$\mathbf{H}_9 = \begin{bmatrix} \mathbf{K}_{22} & \vdots & 0 \\ \dots & \dots & \dots \\ 0 & \vdots & -\mathbf{G}_{22} \end{bmatrix}, \quad \mathbf{H}_{10} = \begin{bmatrix} \mathbf{K}_{13} - \mathbf{K}_{31} & \vdots & -\mathbf{K}_{m\theta 1} \\ \dots & \dots & \dots \\ 0 & \vdots & 0 \end{bmatrix},$$

$$\mathbf{H}_{11} = \begin{bmatrix} \mathbf{K}_{23} - \mathbf{K}_{32} & \vdots & -\mathbf{K}_{m\theta 2} \\ \dots & \dots & \dots \\ 0 & \vdots & 0 \end{bmatrix}, \quad \mathbf{H}_{12} = \begin{bmatrix} -\mathbf{K}_{33} & \vdots & -\mathbf{K}_{m\theta 3} \\ \dots & \dots & \dots \\ 0 & \vdots & \mathbf{G}_{33} \end{bmatrix}.$$

- ¹J. Nowinski, *Theory of thermoelasticity with Applications* (Sijthoff & Noordhoff International, Alphen Aan Den Rijn, 1978).
- ²A. N. Abd-alla and A. A. S. Al-dawy, *Int. J. Math. Math. Sci.* **23**, 529 (2000).
- ³J. D. Achenbach, *Wave Propagation in Elastic Solids* (Elsevier, New York, North-Holland, Amsterdam, 1975).
- ⁴H. W. Lord and Y. Shulman, *J. Mech. Phys. Solids* **15**, 229 (1967).
- ⁵A. E. Green and K. A. Lindsay, *J. Elast.* **2**, 1 (1972).
- ⁶A. E. Naghdi and K. A. Lindsay, *J. Therm. Stresses* **15**, 253 (1992).
- ⁷R. B. Hetnarski and J. Ignaczak, *J. Therm. Stresses* **22**, 451 (1999).
- ⁸A. H. Nayfeh and S. Nemat-Nasser, *Acta Mech.* **12**, 53 (1971).
- ⁹H. Sinha and S. B. Sinha, *Acta Mech.* **23**, 159 (1975).
- ¹⁰Y. Agarwal, *J. Elast.* **8**, 171 (1978).
- ¹¹H. H. Sherief and K. A. Helmy, *J. Therm. Stresses* **22**, 897 (1999).
- ¹²A. N. Abd-alla and A. A. S. Al-dawy, *J. Therm. Stresses* **24**, 367 (2001).
- ¹³C. V. Massalas, *Acta Mech.* **65**, 51 (1986).
- ¹⁴M. Daimaruya and M. Naitoh, *J. Sound Vib.* **117**, 511 (1987).
- ¹⁵C. V. Massalas and V. K. Kalpakidis, *Int. J. Eng. Sci.* **25**, 1207 (1987).
- ¹⁶J. N. Sharma, D. Singh, and R. Kumar, *J. Acoust. Soc. Am.* **108**, 848 (2000).
- ¹⁷J. N. Sharma and P. K. Sharma, *J. Therm. Stresses* **25**, 169 (2002).
- ¹⁸J. C. Cheng and S. Y. Zhang, *Appl. Phys. Lett.* **74**, 2087 (1999).
- ¹⁹Y. C. Fung and P. Tong, *Classical and Computational Solid Mechanics* (World Scientific, Singapore, 2001).
- ²⁰V. T. Buchwald, *Q. J. Mech. Appl. Math.* **14**, 35 (1961).
- ²¹R. Vogelgesang, M. Grimsditch, and J. S. Wallace, *Appl. Phys. Lett.* **76**, 982 (2000).
- ²²G. A. Swift, E. Üstündag, M. A. M. Bourke Bjorn Clausen, and H. -T. Lin, *Appl. Phys. Lett.* **82**, 1039 (2003).
- ²³M. Kitayama, K. Hirao, M. Toriyama, and S. Kanzaki, *J. Am. Ceram. Soc.* **82**, 3105 (1999).
- ²⁴H. Yokota and M. Ibukiyama, *J. Am. Ceram. Soc.* **86**, 197 (2003).
- ²⁵M. Chester, *Phys. Rev.* **131**, 2013 (1963).
- ²⁶J. H. Prevost and D. Tao, *J. Appl. Mech.* **50**, 817 (1983).
- ²⁷A. F. Khadrawi, M. A. Al-Nimr, and M. Hammad, *Int. J. Thermophys.* **23**, 581 (2002).
- ²⁸M. A. Hawwa and A. H. Nayfeh, *J. Appl. Phys.* **80**, 2733 (1996).